PHYSICAL REVIEW D VOLUME 18, NUMBER 9 1 NOVEMBER 1978

Calorimeter triggers for hard collisions

P. V. Landshoff and J. C. Polkinghorne
Department of Applied Mathematics and Theoretical Physics, University of Cambridge, Cambridge, CB 3 9EW, England
(Received 19 January 1978)

We discuss the use of a forward calorimeter to trigger on hard hadron-hadron collisions. We give a derivation in the covariant parton model of the Ochs-Stodolsky scaling law for single-hard-scattering processes, and investigate the conditions when instead a multiple-scattering mechanism might dominate. With a proton beam, this mechanism results in six transverse jets, with a total average multiplicity about twice that seen in ordinary events. We estimate that its cross section is likely to be experimentally accessible at values of the beam energy in the region of 100 GeV/c.

I. INTRODUCTION

Most strong-interaction events are soft, multiperipheral collisions, but in recent years interest has turned to the hard collisions. In these events, the two initial hadrons collide head-on, so that there is a prospect of obtaining information about the inner quark structure of the hadrons and about the way in which the quarks interact with one another.

Most of the investigation of the hard collisions has been through large-transverse-momentum reactions, using single large-p_T particles as triggers. It was realized[1] that a calorimeter would be a more fruitful trigger for large-p_T events, and on the basis of correlation data from the CERN ISR it was predicted[2] that for a given p_T the event rate would be two orders of magnitude times that with a single-particle trigger. There are now experimental indications that this is indeed the case.[3]

In these large-p_T experiments, the calorimeter has limited solid angle and is placed to one side of the beam so as to trigger on those events in which an unusually large transverse momentum or energy is produced in the form of a jet. In an important paper,[4] Ochs and Stodolsky have pointed out the interest of using other types of calorimeter trigger to explore the hard collisions. The information so obtained will be complementary to that from the more conventional high-p_T experiments, and because of the complications in those experiments from trigger bias,[5] some of it may be simpler to interpret.

The original expectation[6] was that hard collisions would be scale-free. This has not so far been found to be the case in high-p_T collisions. A number of possible reasons have been advanced for this,[5] and so far it is not known whether the presence of a mass or length scale is intrinsic to hard collisions, or whether instead collisions that are rather harder, and therefore rarer, than those studied so far will turn out to be scale-free. Another possible point of view (though one which we believe to be less plausible) is that the scale-free character of the reactions has so far been hidden as a result of trigger-bias effects, and one motivation[4] for using new configurations of calorimeter trigger is to attempt to minimize these effects.

Ochs and Stodolsky[4] have discussed the case of a single downstream calorimeter, and they have required that a given fraction τ of the initially forward-going energy is deposited in it. If little energy emerges in the forward direction, there must instead be an appreciable amount of transverse energy. It will be interesting to discover whether this transverse energy emerges in the form of a small number of jets, or whether it is more uniformly distributed in azimuthal angle. The latter possibility would occur, for example, in a model where the two initial hadrons coalesce in their head-on collision so as to form a massive fireball, which then decays isotropically.[7] This is not necessarily ruled out by the fact that a pair of transverse jets appears to be a feature of the conventional high-p_T experiments: it is possible that the triggering configuration in these experiments preferentially selects those events that do contain jets.

But if one assumes that such a trigger does select events in which there is a single pair of transverse jets, and that these are produced by a scale-free hard scattering, then a simple scaling law obtains. This was first stated by Ochs and Stodolsky.[4] We review it in Sec. II, and in the Appendix we show how to derive it from the covariant parton model. We also give the straightforward generalization to the case where the hard scattering that produces the pair of jets is not scale-free.

The Ochs-Stodolsky scaling law applies to the case where the forward-going fractional energy τ in the center-of-mass frame is small, so that it is guaranteed by the kinematics that neither of the transverse jets enters the calorimeter.

Another case of interest, which we discuss in Sec. II, is that in which $\tau > 1$, that is, rather more energy emerges in the forward direction than entered towards that direction. (We work throughout in the center-of-mass frame.) In this case one can be sure that both transverse jets go into the calorimeter, and we give the corresponding scaling law.

It is of interest also to consider the case in which, instead of requiring that the energy E deposited in the calorimeter is less than some fixed fraction τ of the initial forward-going energy, rather E is required to be less than some fixed value E_0. We discuss this in Sec. III. We find that the cross section then receives a contribution from a multiple-scattering effect[8] with the same s dependence, in the case of scale-free scattering, as that obtained from the single-scattering term. This multiple scattering corresponds to each of the valence quarks in the beam particle undergoing a wide-angle hard scatter, with no residual beam fragments. We show that the multiple scattering dominates over the single scattering if the value fixed for E_0 is sufficiently small. Its dominance is further enhanced if there is in addition a calorimeter in the backward direction, and it is required that the energy deposited also in this calorimeter is less than some fixed value. An alternative to this, which may be more practicable, is to have a calorimeter that encompasses 2π in azimuthal angle and includes all but the forward and backward regions. The trigger in this case would be the requirement that all, or very nearly all, the incoming energy was deposited in the calorimeter.

In the multiple-scattering mechanism, the energy is carried off transversely by a number of jets, four in the case of a pion beam and six for a proton beam. These are distributed more or less axisymmetrically about the beam axis. We estimate that, in the case of a 100-GeV/c proton beam, the total average multiplicity will be about twice that seen in ordinary events at the same energy.[9]

In Sec. IV we attempt to give quantitative estimates of the cross section for the multiple-scattering mechanism. These estimates are subject to very considerable uncertainty. For a proton beam, the cross section is an integral of an expression of the form

$$P^2\frac{(\sigma_{qq})^3}{R^4}. \tag{1.1}$$

Here, σ_{qq} is the wide-angle quark-quark scattering cross section, R is a radius that characterizes the proton wave function, and P is the probability that a proton can be a system of three quarks only. We take $R = (140\ \text{MeV})^{-1}$ and argue that comparison with recent pp elastic-scattering data then gives an acceptable value of P. The integration to be performed on (1.1) is one over angles and over the fractional momentum taken by each quark in the beam and target nucleons. We have assumed that the nucleon wave function is peaked very sharply around a value of $\frac{1}{3}$ for the fractional momentum of each quark; making this assumption gives an underestimate of the cross section, quite possibly by an order of magnitude. For σ_{qq}, we use the (non-scale-free) expression that was deduced by Field and Feynman[10] from single-particle large-p_T data:

$$\frac{d\sigma_{qq}}{d\hat{t}} = \frac{\lambda}{-\hat{s}\hat{t}^3}, \quad \lambda = 2300\ \text{mb GeV}^6. \tag{1.2}$$

This gives a multiple-scattering cross section that varies with the incident beam momentum as p^{-9}, and which is of the order of half a millibarn for $p = 100$ GeV/c and a forward calorimeter of acceptance $\pm 45°$ in θ.

However, we must warn that there are reasons to question[5] whether existing large-p_T data can in fact be interpreted in terms of quark-quark scattering. If instead quark-quark scattering is taken to be scale-free, the resulting multiple-scattering cross section falls only as p^{-3}, but its value at $p = 100$ GeV/c is likely to be several orders of magnitude smaller. This last estimate is on the basis that the quark-quark scattering is then described not by (1.2), but occurs through the exchange of a colored octet gluon with point coupling:

$$\frac{d\sigma_{qq}}{d\hat{t}} = \frac{4\pi\alpha_s^2}{9}\frac{\hat{s}^2+\hat{u}^2}{\hat{s}^2\hat{t}^2}. \tag{1.3}$$

[In both (1.2) and (1.3) there should, of course, be additional $\hat{u}$-channel exchange terms if the quarks have the same flavor and color.]

II. OCHS-STODOLSKY SCALING

Suppose that a calorimeter is placed axisymmetrically in the forward direction (Fig. 1). We work throughout in the center-of-mass frame. Let the calorimeter be such as to accept any particle whose angle of emergence θ is less than α, and suppose that in a given event the total energy deposited in the calorimeter is E.

In soft-scattering events, one expects to find that, unless α is very small, $E \approx \frac{1}{2}\sqrt{s}$. Possible triggers that might select the hard-scattering events are thus either $E \ll \frac{1}{2}\sqrt{s}$ or E rather greater than $\frac{1}{2}\sqrt{s}$.

Suppose, to begin with, that the energy is carried away by a single pair of transverse jets, so that one may use a hard-scattering model such as

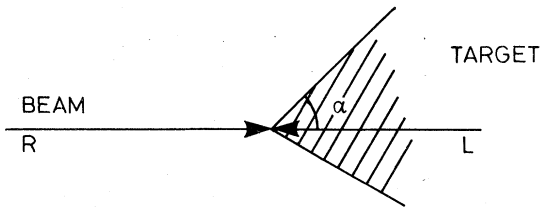

FIG. 1. Downstream veto calorimeter in the center-of-mass frame.

appears[5] to describe conventional high-p_T events. Write

$$\tau = 2E/\sqrt{s}\ . \tag{2.1}$$

We show in the Appendix that if $\alpha < 60°$ and

$$\tau < \tfrac{1}{2}\sec^2(\tfrac{1}{2}\alpha)\,, \tag{2.2}$$

or if α is between 60° and 90° and

$$\tau < \frac{2\sin\frac{1}{2}\alpha}{1+\sin\frac{1}{2}\alpha}\,, \tag{2.3}$$

then it is guaranteed by kinematics that neither jet enters the calorimeter. (This neglects the transverse momenta of the jet fragments relative to their jet axis, which[4] is not a very accurate approximation unless the jet is rather energetic.)

Suppose that one of these pairs of inequalities is satisfied. Then τ is equal to the fractional energy carried by the spectator partons of the initial right-moving hadron:

$$\tau = 1 - x_R\,. \tag{2.4}$$

Here, x_R is the fractional energy taken by the active parton of that hadron, that is the one that undergoes a wide-angle scattering (Fig. 2). As is

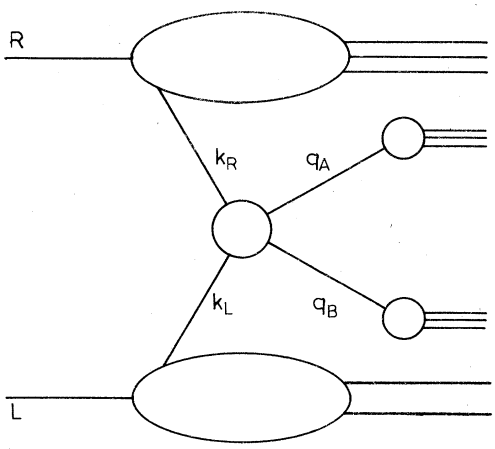

FIG. 2. The single-hard-scattering model.

stated by Ochs and Stodolsky,[4] if this scattering is scale-free,

$$\frac{d\sigma}{d\tau} = \frac{1}{s}\frac{f_R(1-\tau)}{1-\tau}G_L(\xi)\,,$$
$$\xi = (1-\tau)\tan^2(\tfrac{1}{2}\alpha)\,, \tag{2.5}$$

where $f_R(x_R)$ is the probability of finding the parton x_R in the beam and the function G_L depends on the structure of the left-moving initial hadron (the target) and on the dynamics of the central scattering in Fig. 2. If this wide-angle scattering is not scale-free, but rather has the behavior

$$16\pi\hat{s}^2\frac{d\sigma}{d\hat{t}} \sim (\hat{s})^{-n}\Phi(\hat{t}/\hat{u})\,, \tag{2.6}$$

with $n > 0$, then further inverse powers of $s(1-\tau)$ appear:

$$\frac{d\sigma}{dt} = \frac{1}{s^{n+1}}\frac{f_R(1-\tau)}{(1-\tau)^{n+1}}G_L(\xi)\,. \tag{2.7}$$

We derive this formula in the Appendix, together with the explicit form of $G_L(\xi)$:

$$G_L(\xi) = \sum \frac{1}{32\pi}\int_\xi^1 dx\ \frac{f_L(x_L)}{x_L^{n+1}}\int_\xi^{x_L/\xi} dX\,\frac{\Phi(X)}{(1+X)^2} \tag{2.8}$$

where $f_L(x_L)$ is the probability of finding the parton x_L in the target and the summation is over the various different parton-parton scatterings that can occur.

Quantitative estimates of $d\sigma/d\tau$ for the scale-free case $n=0$ have been given by Ochs and Stodolsky. If the quark-quark scattering occurs through the exchange of a colored octet gluon, as in (1.3) with $\alpha_s = \frac{1}{3}$, then for $\tau = \frac{1}{2}$ and $\alpha = 45°$ one finds a value for $d\sigma/d\tau$ at the level of a few microbarns with a 100-Gev/c beam. But the p_T^{-8} behavior so far observed in large-p_T experiments corresponds rather to $n=2$, and with the Field-Feynman form (1.2) for $d\sigma_{qq}/d\hat{t}$ we find that $d\sigma/d\tau$ is nearly two orders of magnitude larger at 100 GeV/c, but it falls more rapidly with increasing beam energy. However, we repeat our warning that the quark-quark scattering interpretation of the large-p_T data may not be correct.

If the inequality (2.2) or (2.3) is not satisfied, one can no longer be sure that neither of the jets enters the calorimeter. However, if

$$\sec^2(\tfrac{1}{2}\alpha) > \tau > \sec^2(\tfrac{1}{4}\alpha)\,, \tag{2.9}$$

then *both* jets will enter the calorimeter, in addition to the beam fragments. Then neither jet is found in the region $\pi > \theta > \frac{1}{2}\alpha$, and so the cross section may be calculated from a straightforward adaptation of (2.7):

$$\frac{d\sigma}{d\tau}=\frac{1}{s^{n+1}}\frac{f_L(\tau-1)}{(\tau-1)^{n+1}}G_R(\zeta)\,,$$
$$\zeta=(\tau-1)\cot^2(\tfrac{1}{2}\alpha)\,. \tag{2.10}$$

The function G_R is as given in (2.8), with f_L replaced by f_R.

Of course, some "ordinary" events will have $\tau > 1$. So, in order to be reasonably sure that by triggering in this way one might be selecting a hard-scattering event, one must take τ rather greater than 1. Because of (2.9), this demands a reasonably large calorimeter. With $\alpha = 60°$ and $\tau = 1.2$, we find that the scale-free wide-angle quark-quark scattering gives a cross section at the 50-nb level for a 100-GeV/c proton beam, while the Field-Feynman scattering gives a value of a few microbarns.

III. FIXED-ENERGY TRIGGERS AND MULTIPLE SCATTERING

The rapid decrease of $d\sigma/d\tau$ as $\tau \to 0$ is due to the decrease of $f_R(1-\tau)$ as $\tau \to 0$. If $f_R(1-\tau)\sim\tau^m$ as $\tau \to 0$, then for sufficiently small $\tau = 2E/\sqrt{s}$ we obtain from (2.7)

$$\frac{d\sigma}{dE}\propto s^{-n-m/2-3/2}E^m\,, \tag{3.1}$$

where E is the energy deposited in the calorimeter. This formula gives the behavior of the cross section for fixed $E \ll \frac{1}{2}\sqrt{s}$.

For a nucleon beam, $m = 3$ or 4. With $m = 3$, and for scale-free scattering ($n = 0$), the cross section $\sigma_p(E_0)$ for the deposit of energy $E \leq E_0$ in the downstream calorimeter has the behavior

$$\sigma_p(E_0)\propto s^{-3}E_0{}^4\,. \tag{3.2}$$

This is calculated from (3.1). There is, however, another process which in the scale-free case gives a contribution to $\sigma_p(E_0)$ with the same s dependence as (3.2) but with a coefficient that does not vanish as $E_0 \to 0$.

This process is the multiple-scattering mechanism, by which all the (valence) quark constituents of the beam proton are scattered at wide angle as shown in Fig. 3. (We have previously considered[8] a similar multiple-scattering mechanism as a possible source of large-p_T baryon production.) Each of the three quarks of the beam proton is scattered at wide angle off a constituent of the other initial-state hadron. After these scatterings the participating partons emerge in different directions to form six jets. In contrast with Fig. 2, where the two transverse jets are coplanar with the intial beam, these six jets are distributed more or less randomly in azimuthal angel (though they are coplanar in pairs with the initial beam).

As we explain in the Appendix, if the three wide-angle scatterings are scale-free the mechanism gives

$$\frac{d\sigma}{d\tau}\sim s^{-3}\delta(\tau)[M_p(\alpha)]^4\,, \tag{3.3}$$

leading on integration to a contribution to $\sigma_p(E_0)$ of the form

$$\sigma_p(E_0)\sim s^{-3}[M_p(\alpha)]^4\,. \tag{3.4}$$

Here $M_p(\alpha)$ is a function that is independent of E_0. It is determined by the wave functions of the two interacting nucleons and by the angular dependences of the wide-angle scatterings, and it has the dimensions of mass.

With a pion beam, only two wide-angle scatterings are necessary. If these are scale-free, one obtains

$$\sigma_\pi(E_0)\sim s^{-2}[M_\pi(\alpha)]^2\,. \tag{3.5}$$

The corresponding result from the single-scattering mechanism is

$$\sigma_\pi(E_0)\propto s^{-2}E_0{}^2\,, \tag{3.6}$$

if $m = 1$ for the pion. In either case, therefore, the multiple scattering gives the same s dependence as the single scattering if the hard scattering is scale-free, and becomes dominant for sufficiently small values of E_0. If, on the other hand, $m = 4$ for the proton, or $m = 2$ for the pion, the single-scattering results, (3.2) or (3.6), will have an additional factor $E_0/\sqrt{s}$, so that then the multiple scattering will become dominant at any fixed E_0 if the energy $\sqrt{s}$ is sufficiently large.

In order to obtain the result (3.3), we have used the part of the wave function of the initial right-moving proton that consists only of valence-quark components, with no additional nonvalence $q\bar{q}$

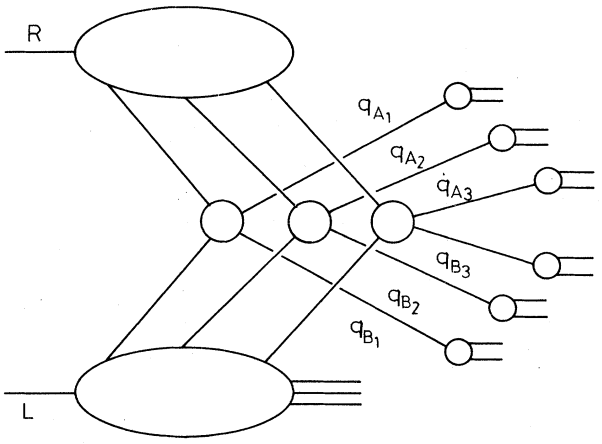

FIG. 3. The multiple-hard-scattering model.

pairs. For the left-moving initial nucleon, we can use the whole wave function. However, if for the left-moving nucleon we use also only the valence part, we obtain a cross section where no energy emerges either forwards or backwards, and all the initial energy is carried off by the six transverse jets. If we integrate, to obtain the cross section for the case where the energy is less than E_0, the result again has the form (3.4), though with a smaller numerical coefficient because now only part of the wave function of the left-moving nucleon is used. On the other hand, the scale-free single-scattering mechanisms in this case would give a contribution proportional to E_0^8/s^5 (assuming $m=3$).

If the wide-angle quark-quark scatterings are not scale-free, but rather $n=2$, then $\sigma_p(E_0)$ and $\sigma_\pi(E_0)$ are still independent of E_0 in the multiple-scattering mechanism. However, now the mechanism gives $\sigma_p(E_0)\propto s^{-9}$ and $\sigma_\pi(E_0)\propto s^{-6}$. The falloff with s is then too rapid to offer any hope that the mechanism may be detectable at very high-energy, However, in the next section we estimate that the cross sections may well be accessible at beam momentum in the region of 100 GeV/c.

IV. QUANTITATIVE ESTIMATES OF MULTIPLE SCATTERING

We do not have sufficient information to calculate the multiple-scattering mechanism with any accuracy. In this section we present rough estimates of the cross section. We use a crude geometrical picture, and exploit the possible connection between the mechanism and Regge cuts.[12] We consider only the nucleon-beam case.

We imagine that each initial nucleon consists of just three valence quarks, and that the wave function is very sharply peaked so that each quark takes $\frac{1}{3}$ of the nucleon momentum. These assumptions greatly simplify the kinematics, since they imply that the overall center-of-mass frame is also the center-of-mass frame for each of the three wide-angle scatterings. This means that we have to integrate $d\sigma_{qq}/d\hat{t}$, given by either (1.2) or (1.3), between $\hat{t}=-\hat{s}\sin^2(\frac{1}{2}\alpha)$ and $\hat{t}=-\hat{s}\cos^2(\frac{1}{2}\alpha)$ in order to ensure that in each scattering both quarks are scattered clear of the forward calorimeter. In the scale-free case (1.3), the result is (to a sufficient degree of accuracy when $\alpha\lesssim 60°$)

$$\sigma_{qq}(\alpha)=\frac{8\pi\alpha_s^{\,2}}{s\sin^2(\frac{1}{2}\alpha)}, \tag{4.1}$$

where we have used $\hat{s}=s/9$. The corresponding answer with the Field-Feynman cross section (1.2) is

$$\sigma_{qq}(\alpha)=\frac{729\lambda}{2s^3\sin^4(\frac{1}{2}\alpha)}. \tag{4.2}$$

If the radius of the nucleon is R, the cross section for head-on collision of the two nucleons is πR^2. When this occurs, the probability that each quark of one nucleon collides with a quark of the other and scatters through the required angle is approximately

$$6\times 4\left(\frac{\sigma_{qq}(\alpha)}{\pi R^2}\right)^3.$$

The factor 6 counts the number of ways the quarks can be paired and the factor 4 approximates the average enhancement due to the existence of $\hat{u}$-channel exchanges for some pairings. [(4.1) and (4.2) have been calculated for $\hat{t}$-channel exchanges. The existence of color makes the exchanges combine in a way that is predominantly incoherent. However, when quarks of the same color and flavor interact, there is destructive interference, which makes 4 a slight overestimate.]

Hence we estimate the cross section for the case where both nucleons consist of three quarks only as

$$\sigma(\alpha)=\frac{24P^2[\sigma_{qq}(\alpha)]^3}{\pi^2R^4}, \tag{4.3}$$

where P is the probability of the three-quark configuration in a nucleon. If we take $R^{-1}=140$ MeV, $\alpha_s=\frac{1}{3}$, and λ given by (1.2), the scale-free case (4.1) gives $\sigma\approx 4P^2\times 10^{-34}$ cm^2 at 100 GeV/c, while the Feynman-Field cross section (4.2) gives about P^2 mb at the same energy. Notice that in the latter case the cross section decreases much more rapidly with increasing s, and with increasing α.

We can test the reasonableness of the picture by seeking to estimate P from pp elastic-scattering data. At very small momentum transfer the differential cross section is, of course, dominated by single Pomeron exchange. We have previously suggested[13] that the Pomeron couples directly and in a simple fashion to the valence quarks within the proton, so that at small t the differential cross section for quark-quark scattering is

$$\frac{d\sigma_{qq}}{d\hat{t}}=\frac{g^4}{16\pi\hat{s}^2}\left(\frac{\hat{s}}{m_p^{\,2}}\right)^{2\alpha_P(\hat{t})-2}. \tag{4.4}$$

We found that a good fit to small-t elastic-pp data was obtained by taking the Pomeron trajectory $\alpha_P(t)$ to have slope $\frac{1}{4}$, and the coupling g approximately constant at the value

$$\frac{g^4}{16\pi}=1\ \text{mb/GeV}^2. \tag{4.5}$$

The pp elastic-scattering data[14] from the ISR show

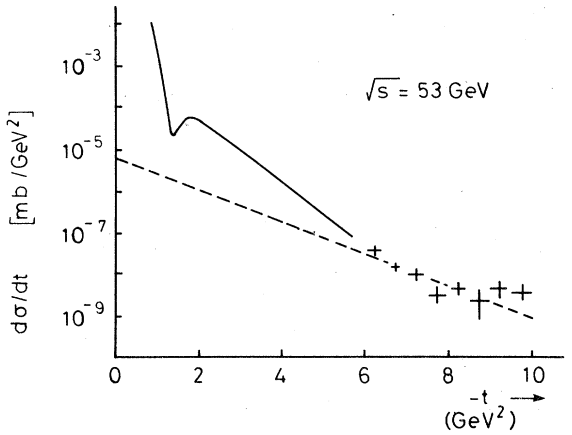

FIG. 4. $d\sigma/dt$ for pp scattering at $\sqrt{s}=53$ GeV.

a dip at $-t=1.34$ GeV^2, followed by a change of slope. It seems reasonable to suppose that this is due to a changeover from single-Pomeron to double-Pomeron exchange. It has now been reported[14] that there is a further change of slope at $-t=6.5$ GeV^2; see Fig. 4. We shall assume that this results from a changeover to triple-Pomeron exchange.[15]

The diagram corresponding to the triple-Pomeron cut is Fig. 5, with each bubble a Pomeron-exchange amplitude. At small t, there will be additional lines joining the two top vertices R, and also joining the two bottom vertices L. However, as $|t|$ increases we expect that the importance of these additional insertions will diminish, since then the quarks k_R' are moving in a rather different direction from the quarks k_R, and similarly

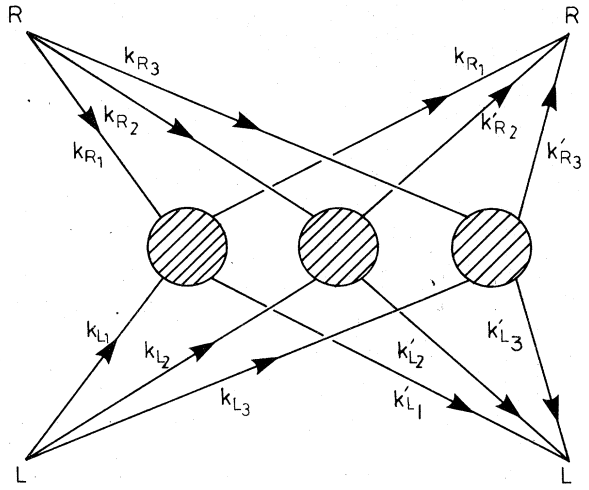

FIG. 5. The squared modulus of the matrix element for multiple scattering—and also the Mandelstam Regge-cut diagram.

for the lower vertices. So if we take the triple-Pomeron-exchange data at reasonably large $|t|$ and extrapolate it back to $t=0$, we expect to obtain the contribution to the triple-Pomeron cut from Fig. 5 with no additional lines inserted. We have performed this extrapolation in Fig. 4, using the best fit 0.88 to the slope quoted by the experimentalists.[14] This extrapolation is, of course, highly uncertain, but an error of an order of magnitude here will give an error of less than a factor of 2 in the estimation of P.

From the extrapolation in Fig. 4,

$$7\times 10^{-6}\ \text{mb/GeV}^2=\frac{1}{16\pi s^2}\,|\mathfrak{M}^{\text{cut}}|^2, \tag{4.6}$$

where $\mathfrak{M}^{\text{cut}}$ is the Regge-cut amplitude at $t=0$. The calculation of this amplitude is described in the Appendix. Because the slope of the Pomeron trajectory $\alpha_P(t)$ is small, we may approximate α_P by the constant value 1. Because of our assumptions about the nucleon-wave function, we may also set $x_{Ri}=x_{Li}=\frac{1}{3}$ in (A13) and (A14). The result is that the squared matrix element for Fig. 3 is

$$|\mathfrak{M}|^2=\left[\frac{2\sigma_{qq}(\alpha)}{g^2}\right]^3\mathfrak{M}^{\text{cut}}. \tag{4.7}$$

As before, we include a factor close to 4 for $\hat{u}$-channel exchanges, and a flux factor $1/(2s)$:

$$\sigma(\alpha)=\frac{16}{s}\,\frac{[\sigma_{qq}(\alpha)]^3}{g^6}\,\mathfrak{M}^{\text{cut}}. \tag{4.8}$$

We compare this with (4.3). Notice first that the energy-dependent quark-quark cross section cancels out between the two expressions, as it should. Using (4.5) and (4.6) and choosing $R^{-1}=140$ MeV, we obtain

$$P=\tfrac{3}{5}. \tag{4.9}$$

Because of the crudeness of our calculations this result should not be interpreted too literally, but we regard it as a reasonable value which sustains confidence in the general approach used.

We have here compared cross sections where both nucleons are treated as three-quark systems. This is in fact the quantity of relevance when there are veto calorimeters both upstream and downstream with the requirement that no energy is deposited in either. When there is only a downstream calorimeter, it is the process represented by Fig. 3 which we wish to calculate, in which the right-moving nucleon is treated as a three-quark system but the left-moving nucleon can have additional structure. It is not possible to calculate this by a Regge-cut comparison, but if we assume that it is crudely estimated by replacing P^2 by P in (4.3), then we obtain the value of $\frac{3}{5}$ mb at 100

Gev/c with the Field-Feynman hard scattering, as quoted in Sec. I.

V. DISCUSSION

We have sought to discuss in this paper the physics of experiments based on downstream calorimeters. For the case of a finite fraction τ of the beam energy deposited in the calorimeter we confirm the Ochs-Stodolsky scaling law, suitably generalized to the nonscaling case as necessary, both for the case of small τ satisfying (2.2) or (2.3) and also for the case of $\tau > 1$. In Sec. II we showed that at 100 GeV/c the Field-Feynman quark scattering would give a cross section two orders of magnitude greater than that given by scale-free gluon exchange with $\alpha_s = \frac{1}{3}$. However, the Field-Feynman contribution will soon damp out compared to the latter as the beam energy increases.

When the case of limited energy deposited in the calorimeter ($E \leq E_0$) is considered, a new multiple-scattering mechanism may be of importance which gives a contribution independent of E_0. We estimate that for a ±45° calorimeter its contribution will only be a fraction of a nanobarn at 100 GeV/c if the hard scatter is gluon exchange with $\alpha_s = \frac{1}{3}$, but if the hard scatter is due to the Field-Feynman process the cross section could be at the half millibarn level at that energy. Moreover, it would not be reduced very substantially if a similar upstream veto calorimeter were also inserted.

Various striking features would be present in events triggered to choose interactions dominated by this multiple-scattering mechanism. One is obviously the presence of six transverse jets, coplanar with the beam only in pairs, though since at 100 GeV/c each jet carries only about 2 GeV energy the appearance of the jets will be rather diffuse, and it is not likely to be possible to separate them from each other. The large number of jets would imply an enhanced multiplicity of secondaries. Using phenomenological inputs for jet multiplicity we estimate this to enhance the associated multiplicity by a factor of about 2 over ordinary events at 100 GeV/c. Because the cross section decreases rapidly with increasing α, in most events three of these jets will lie just outside the veto calorimeter. (The same effect occurs also for one of the pair of jets from the single-scattering mechanism.) This fact means however that the transverse momenta of jet fragments relative to their jet axis, which we have not taken into account, must have some significance for detailed estimating of cross sections, as Ochs and Stodolsky have warned.

Finally, we comment on our choice of 100 Gev/c as beam momentum in calculation. Owing to the rapid decrease of cross sections with s (particularly for the case of the nonscaling Field-Feynman interaction) it is necessary to choose the momentum not too large if observable effects are to be found. On the other hand the beam momentum must not be chosen too small, for otherwise the hard-scattering approximation breaks down. This is signaled by the rapid increase of cross section with decreasing s. Of course this increase is cut off eventually by the unknown subasymptotic behavior of the quark scatterings. 100 GeV/c gives an energy of somewhat over 2 GeV/jet, which seems the smallest plausible value for which to use the theory.

APPENDIX

The single-scattering term

In order to calculate the diagram of Fig. 2, we parametrize the momentum four-vector of each transverse jet in terms of its transverse component $\frac{1}{2}x_T\sqrt{s}$, its pseudorapidity η, its azimuthal angle ϕ and its total invariant mass m:

$$q_a = \tfrac{1}{2}x_{Ta}\sqrt{s}\left(\cosh\eta_a + \frac{2m_a^2}{sx_{Ta}^2\cosh\eta_a}, \cos\phi_a, \sin\phi_a, \sinh\eta_a\right), \quad a = A, B. \tag{A1}$$

This parametrization is valid asymptotically. For the initial parton momenta, we use our usual[12] parametrizations

$$\begin{aligned} k_R &= (\tfrac{1}{2}x_L\sqrt{s} + y_R/\sqrt{s}, \kappa_R, \tfrac{1}{2}x_R\sqrt{s}), \\ k_L &= (\tfrac{1}{2}x_L\sqrt{s} + y_L/\sqrt{s}, \kappa_L, -\tfrac{1}{2}x_L\sqrt{s}), \end{aligned} \tag{A2}$$

where κ_R and κ_L are two-dimensional vectors transverse to the beam direction.

We have to integrate over q_A, q_B, k_R, and k_L. In terms of our parameters,

$$\begin{aligned} \int d^4q_a &= \tfrac{1}{8}s\int x_{Ta}dx_{Ta}d\eta_a d\phi_a dm_a^2, \quad a = A, B \\ \int d^4k_b &= \tfrac{1}{2}\int dx_b dy_b d^2\kappa_b, \quad b = R, L. \end{aligned} \tag{A3}$$

These integrations are constrained by δ functions that conserve the four-momentum in the central scattering: asymptotically,

$$\begin{aligned} &\delta^{(4)}(k_R + k_L - q_A - q_B) \\ &\sim \frac{8}{x_{TA}s^2}\delta(\phi_A - \phi_B + \pi)\delta(x_{TA} - x_{TB}) \\ &\times \delta(x_R - \tfrac{1}{2}x_{TA}(e^{\eta_A} + e^{\eta_B}))\delta(x_L - \tfrac{1}{2}x_{TA}(e^{-\eta_A} + e^{-\eta_B})). \end{aligned} \tag{A4}$$

We shall write $x_{TA} = x_{TB} = x_T$.

The variables associated with the central hard scattering are

$$\hat{s} = (k_R + k_L)^2 \sim x_R x_L s \,,$$
$$\hat{t} = (k_R - q_1)^2 \sim -x_R x_T s e^{-\eta_A} \,, \tag{A5}$$
$$\hat{u} = (k_R - q_2)^2 \sim -x_R x_T s e^{-\eta_B} \,.$$

We asume that the corresponding matrix element satisfies the scaling law as in (2.6),

$$|\mathfrak{M}_{qq}|^2 \sim (\hat{s})^{-n} \Phi(\hat{t}/\hat{u}) \,, \tag{A6}$$

with $n = 0$ if the scattering is scale-free. [In (A6) we have suitably summed an averaged over parton spins].

When (A1) to (A8) are used in the integral for the cross section associated with Fig. 2, various parts of the integral decouple. The variables y_R and κ_R appear only associated with the top bubble, and the subintegral over them is[12] proportional to the parton probability distribution $f_R(x_R)$. Similarly, the y_L and κ_L integrations give a contribution proportional to $f_L(x_L)$. The ϕ_A and ϕ_B integrations over the azimuthal angle are, of course, trivial. The variables $m_A{}^2$ and $m_B{}^2$ appear only as arguments of the spectral functions for the two transverse jets, and so the integration over each of these variables gives unity.

With a flux factor $(2s)^{-1}$, we have therefore

$$\sigma = \sum \frac{1}{64\pi s^{n+1}} \int d\eta_A \, d\eta_B \, x_T \, dx_T \, dx_R \, dx_L \frac{f_R(x_R) f_L(x_L)}{(x_R x_L)^{n+1}} \tag{A7}$$
$$\times \Phi(e^{\eta_B - \eta_A}) \delta(x_R - \tfrac{1}{2} x_T (e^{\eta_A} + e^{\eta_B})) \delta(x_L - \tfrac{1}{2} x_T (e^{-\eta_A} + e^{-\eta_B})) \,,$$

where the summation is over the various parton-parton scatterings that can occur. To calculate $d\sigma/d\tau$, we insert under the integral the extra factors

$$\delta(1 - \tau - x_R) \theta(e^{-\eta_A} - \tan\tfrac{1}{2}\alpha) \theta(e^{-\eta_B} - \tan\tfrac{1}{2}\alpha)$$

and introduce the integration variable

$$X = \frac{x_R}{x_L} e^{-2\eta_A} \,. \tag{A8}$$

This leads to the result (2.8).

In order to derive the inequalities (2.2) and (2.3), notice first that it is trivial to show from the kinematics that if both jets enter the calorimeter then necessarily $\tau > 1$. So, suppose that $\tau < 1$ and that one jet enters the calorimeter. Let this be the jet q_A. Then, from (A1),

$$\tau = 1 - x_R + x_T \cosh\eta_A$$
$$= 1 - x_R \frac{e^{\eta_B} - e^{-\eta_A}}{e^{\eta_B} + e^{\eta_A}} \,, \tag{A9}$$

where we have used the first δ function in (A7). A straightforward calculation shows that the minimum value of τ occurs for $x_R = 1$, $e^{\eta_B} = \cot\frac{1}{2}\alpha$, and

$$e^{\eta_A} = \cot\tfrac{1}{2}\alpha \quad \alpha < 60^\circ$$
$$= \sec\tfrac{1}{2}\alpha + \tan\tfrac{1}{2}\alpha \quad 60^\circ < \alpha < 90^\circ \,. \tag{A10}$$

If τ is less than this minimum value, we can be sure that neither jet enters the calorimeter; this gives the conditions (2.2) and (2.3).

Multiple scattering

The calculation of the multiple-scattering term of Fig. 3 is more complicated. This is partly because, while in the case of the single scattering (Fig. 2) the internal momenta are determined when the external momenta are prescribed, this is not true for multiple scattering. This means that when we calculate the squared modulus $\mathfrak{M}\mathfrak{M}^*$ of the matrix element, the internal momenta in $\mathfrak{M}$ and $\mathfrak{M}^*$ are not exactly equal. We draw $\mathfrak{M}\mathfrak{M}^*$ in Fig. 5, and show how we label the momenta. Here, each of the three central bubbles represents a suitable integral of the squared matrix element $\mathfrak{M}_{qq}\mathfrak{M}_{qq}^*$ for quark-quark scattering: we illustrate this in Fig. 6, where we show a $\hat{t}$-channel exchange. The lines q_A, q_B are the transverse jets of Fig. 3.

We parametrize each internal parton momentum k_R, k_R', k_L, and k_L' as in (A2). For each momentum, the Jacobian of the transformation is $\frac{1}{2}$: see the second equation of (A3). These momenta are constrained by energy-momentum conservation at the external vertices R, L. If the vertex has no additional beam fragments, as is the case for the R vertex in Fig. 3, we obtain

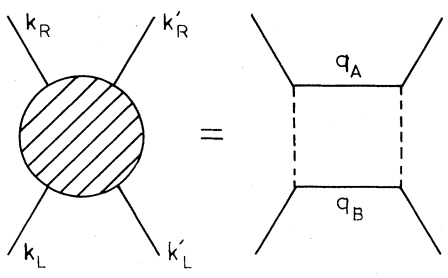

FIG. 6. Hard scattering by exchange in the $\hat{t}$ channel (to be inserted into Fig. 5).

$$4\delta\left(\sum_{i=1}^{3} x_{bi}-1\right)\delta\left(\sum_i x'_{bi}-1\right)\delta\left(\sum_i y_{bi}\right)\delta\left(\sum_i y'_{bi}\right)$$
$$\times\delta^{(2)}\left(\sum_i \underset{\sim}{\kappa}_{bi}\right)\delta^{(2)}\left(\sum_i \underset{\sim}{\kappa}'_{bi}\right) \quad \text{(A11a)}$$

from that vertex b. If there are aditional beam fragments, as for the L vertex in Fig. 3, these must have the same total momentum for $\mathfrak{M}$ and $\mathfrak{M}^*$, and so we have instead of (A11a),

$$2\delta\left(\sum_i x_{bi}-\sum_i x'_{bi}\right)\delta\left(\sum_i y_{bi}-\sum y'_{bi}\right)$$
$$\times\delta^{(2)}\left(\sum_i \underset{\sim}{\kappa}_{bi}-\sum_i \underset{\sim}{\kappa}'_{bi}\right). \quad \text{(A11b)}$$

Then there is energy-momentum conservation for each of the bubbles in Fig. 5. Because of (A11), if we impose this for two of the bubbles, it will automatically be satisfied for the third one. Hence we have

$$\prod_{i=1}^{2}\frac{2}{s}\delta(x_{Ri}-x'_{Ri})\delta(x_{Li}-x'_{Li})\delta^{(2)}(\underset{\sim}{\kappa}_{Ri}+\underset{\sim}{\kappa}_{Li}-\underset{\sim}{\kappa}'_{Ri}-\underset{\sim}{\kappa}'_{Li}). \quad \text{(A12)}$$

For each of the bubbles in Fig. 5, we parametrize the momenta q_A, q_B (displayed in Fig. 6) as in (A1). Energy-momentum conservation within each bubble gives δ functions as in (A4), and for each momentum q_A, q_B the transformation of integration variables requires a Jacobian as in the first equation of (A3). The powers of s from (A4) and Jacobian cancel, so that if the wide-angle quark-quark scattering is scale-free, the overall power of s in $|\mathfrak{M}|^2$ comes from (A12) and is s^{-2}. With a flux factor, this gives an s^{-3} behavior for the cross section.

With a further transformation of integration variable as in (A8), we find that the contribution from each bubble is

$$\frac{2\pi^3}{(x_{Ri}x_{Li})^{n+1}}\int_{\xi_i/x_{Li}}^{x_{Li}/\xi_i} dX_i\,\frac{\Phi(X_i)}{(1+X_i)^2},$$

$$\xi_i = x_{Ri}\tan^2(\tfrac{1}{2}\alpha). \quad \text{(A13)}$$

The remaining factors in the integral corresponding to Fig. 5 are the vertex functions, corresponding to the vertices R and L. In Sec. IV we make use of the fact that the same vertex functions come into the calculation[12] of the triple-Regge cut in the pp-scattering amplitude at zero-momentum transfer. That is, if we replace each of the bubbles by a simple Regge exchange, we obtain just the Mandelstam-cut diagram.[12] In this case, (A13) is replaced by

$$(2\pi)^4 g^2\left(\frac{\hat{s}_i}{m_p^2}\right)^{\alpha_P(\underset{\sim}{\chi}_i^2)}, \quad \text{(A14)}$$

$$\hat{s}_i = x_{Ri}x_{Li}s, \quad \underset{\sim}{\chi}_i = \underset{\sim}{\kappa}_{Ri}-\underset{\sim}{\kappa}'_{Ri},$$

where α_P is the Regge trajectory and g is its coupling to the quarks.

[1] J. D. Bjorken, Phys. Rev. D 8, 4098 (1973).

[2] S. D. Ellis, M. Jacob, and P. V. Landshoff, Nucl. Phys. B108, 93 (1976); M. Jacob and P. V. Landshoff, Nucl. Phys. B113, 395 (1976).

[3] C. Bromberg *et al.*, Phys. Rev. Lett. 38, 1447 (1977).

[4] W. Ochs and L. Stodolsky, Phys. Lett. 69B, 225 (1977).

[5] For recent review, see P. V. Landshoff, talks at Workshops at Bielefeld and CERN, Cambridge Report No. DAMTP 77/28 (unpublished); J. C. Polkinghore, in *Proceedings of the 1977 European Conference on Particle Physics, Budapest*, edited by L. Jenik and I. Montvay (Central Research Institute for Physics, Budapest, Hungary, 1977); C. Michael, Liverpool report (unpublished).

[6] S. M. Berman, J. D. Bjorken, and J. Kogut, Phys. Rev. D 4, 3388 (1971).

[7] References to this type of model were given by P. V. Landshoff, in *Proceedings of the XVII International Conference on High Energy Physics, London*, 1974, edited by J. R. Smith (Rutherford Laboratory, Chilton, Didcot, Berkshire, England, 1974), p. V-57.

[9] P. V. Landshoff, J. C. Polkinghorne, and D. M. Scott, Phys. Rev. D 12, 3728 (1975).

[9] For measurements of jet multiplicities, see for example, the data of the Pisa–Stony Brook collaboration, R. Kephart *et al.*, Phys. Rev. D 14, 2909 (1976).

[10] R. Field and R. Feynman, Phys. Rev. D 15, 2590 (1977).

[11] Our estimates fall more than two orders of magnitude below those of Ref. 4. The reason appears to lie in a number of factors: we take $\alpha_s = \frac{1}{3}$ rather than 1; we take into account color and the different flavors of partons; we use a different, and we believe more realistic quark probability function [namely $3(1-x)^4$].

[12] See the review by P. V. Landshoff and J. C. Polkinghorne, Phys. Rep. 5C, 1 (1972).

[13] P. V. Landshoff and J. C. Polkinghorne, Nucl. Phys. B32, 541 (1971); G. A. Jaroszkiewicz and P. V. Landshoff, Phys. Rev. D 10, 170 (1974); F. Ravndal, Phys. Lett. 37B, 300 (1971).

[14] H. De Kerret *et al.*, Phys. Lett. 68B, 374 (1977).

[15] See H. A. Neal and H. B. Nielsen, Phys. Lett. 51B, 79 (1974). The validity of this assumption is disputed in a recent paper by P. D. Collins and F. Gault, Durham report (unpublished).